

Theoretical foundations of quantum hydrodynamics for plasmas

Zh. A. Moldabekov^{1,2,3}, M. Bonitz¹, and T. S. Ramazanov^{2,3}

¹*Institut für Theoretische Physik und Astrophysik,*

Christian-Albrechts-Universität zu Kiel, Leibnizstraße 15, 24098 Kiel, Germany

²*Institute for Experimental and Theoretical Physics, Al-Farabi Kazakh National University,*
71 Al-Farabi str., 050040 Almaty, Kazakhstan and

³*Institute of Applied Sciences and IT, 40-48 Shashkin Str., 050038 Almaty, Kazakhstan*

Beginning from the semiclassical Hamiltonian, the Fermi pressure and Bohm potential for the quantum hydrodynamics application (QHD) at finite temperature are consistently derived in the framework of the local density approximation with the first order density gradient correction. Previously known results are revised and improved with a clear description of the underlying approximations. A fully non-local Bohm potential, which goes beyond of all previous results and is linked to the electron polarization function in the random phase approximation, for the QHD model is presented. The dynamic QHD exchange correlation potential is introduced in the framework of local field corrections, and considered for the case of the relaxation time approximation. Finally, the range of applicability of the QHD is discussed.

PACS numbers: xxx

I. INTRODUCTION

The investigation of dynamical properties of systems containing partially or fully degenerate electrons has gained growing interest due to their relevance for such fields like dense plasmas [1, 2], warm dense matter [3, 4], streaming and wake effects [5, 6] and plasmonics [7–10]. Interiors of giant planets, white and brown dwarfs, stellar cores, and the outer envelope of neutron stars are examples of matter in the state of a partially degenerate dense plasma (warm dense matter) [11, 12]. Experimental studies of dense plasmas include the free electron laser excited plasmas [13], and inertial confinement fusion experiments [14–16]. On the other hand, plasmonic materials, containing fully degenerate electrons, have recently received renewed attention as the result of the advances in nanofabrication techniques [8, 9, 17, 18]. All the above mentioned different systems are governed by the behavior of Coulomb interacting quantum electrons.

The theoretical description of quantum plasmas must take into account quantum degeneracy effects such as non-locality, spin statistics, and correlations (non-ideality) appropriately on the relevant scales. A continuum description of the dynamics of the quantum electrons in the spirit of a density functional theory (DFT) is a promising approach to the problem. The possibility of such a description follows from the Hohenberg-Kohn theorem of DFT [21, 22] and the Runge-Gross theorem of time-dependent (or current) density functional theory (TDDFT) [23]. The dynamics of the electrons can be described in terms of the average electron density $n(\mathbf{r}, t)$ and the average electron current density $\mathbf{j}(\mathbf{r}, t)$ by the continuity and momentum equations [19, 23]:

$$\frac{\partial}{\partial t} n(\mathbf{r}, t) + \nabla \cdot [\mathbf{j}(\mathbf{r}, t)] = 0, \quad (1)$$

$$m \frac{\partial}{\partial t} \mathbf{j}(\mathbf{r}, t) - n(\mathbf{r}, t) e \mathbf{E}(\mathbf{r}, t) = -\nabla \cdot \mathbf{P}(\mathbf{r}, t), \quad (2)$$

where \mathbf{E} is the electric-field strength, and \mathbf{P} stands for a tensor that contains all many-body and quantum effects, including correlations and dissipation. The exact form of \mathbf{P} is not known, and different approaches and approximations for \mathbf{P} have been proposed with different levels of sophistication, e.g. [24, 25].

An alternative concept are first-principle approaches based on wave function methods, e.g. [26], quantum-statistical theory [1], quantum kinetic theory [20, 27] or non-equilibrium Green functions [28, 29]. However, as TDDFT, these methods require substantial theoretical and computational effort and are particularly important to capture electronic correlations. Therefore, in cases where correlations and their dynamics are of minor importance, simpler approaches are being used. This particularly applies to quantum hydrodynamics (QHD) that became popular as a simplified approach for quantum plasmas [30–34], plasmonics [8–10, 35], and electrons in semiconductors [36, 37] and is, therefore, in the focus of this paper.

The key ingredients of QHD – as it is often used in the context of quantum plasmas – are the ideal Fermi pressure, P_F , and the so-called Bohm potential, V_B [38]. In QHD, the closed momentum equation is, instead of Eq. (2),

$$m \frac{\partial}{\partial t} \mathbf{j}(\mathbf{r}, t) - n(\mathbf{r}, t) e \mathbf{E}(\mathbf{r}, t) = -\nabla P_F[n(\mathbf{r}, t)] - n(\mathbf{r}, t) \nabla V_B[n(\mathbf{r}, t)], \quad (3)$$

Manfredi and Haas [31] derived the Fermi pressure and a quantum correction in the form of the Bohm potential using a semi-classical Hartree ansatz for the N -electron wave functions with identical amplitude for all single-electron orbitals [38]. However, in order to reach agreement with the results of the more fundamental kinetic theory in its simplest form – the random phase approximation (RPA) – both, the Fermi pressure and the Bohm potential have to be “corrected” by constant pre-factors

[35, 43–45]. Similarly, in plasmonics, the QHD theory is used with one or, sometimes, two fitting parameters corresponding to the prefactors of the Fermi pressure and the Bohm potential, but with an additional exchange correlation potential contribution, which is valid only in the static case.

Moreover, in the context of quantum plasmas, QHD has often been used beyond the range of applicability of the model and, occasionally, even with explicitly incorrect expressions. This has led to un-physical predictions and some controversy, for a discussion, see Refs. [38–41, 48].

However, introducing the above mentioned corrections factors does not solve the problem. It turned out that these fitting parameters (pre-factors) are not constants but differ depending on the characteristic wavelength and frequency of the physical problem. In addition, these coefficients are found to vary with the plasma density and temperature. This results in complicated parametric dependencies of the Bohm potential. This means that the range of the values in which correcting parameters can be chosen and the corresponding underlying physical assumptions need to be clarified.

For this reason, in this paper QHD is reconsidered in detail, for both zero temperature and finite temperature, and it is put into the context of well established approaches such as Thomas-Fermi theory and dielectric theory (such as the random phase approximation). Starting from these approaches it becomes more clear what approximations are actually being made and what is the corresponding range of validity of the model.

In Sec. II, continuity and momentum equations of the QHD model are briefly introduced for the finite temperature case. In Sec. III, the relation of the Bohm potential in the density gradient approximation to the power expansion of the inverse finite temperature RPA polarization function is presented, and the QHD potentials, i.e., the potential related to the Fermi pressure and the Bohm potential, are considered in different limiting cases. This will allow us to reproduce known results and, in part, even to improve them. In Sec. IV, the generalized non-local Bohm potential, based on the exact RPA polarization function, is presented. The exchange-correlation potential for the QHD application is discussed in Sec. V. The paper is concluded by a discussion of the range of applicability of the QHD model.

II. QHD EQUATIONS AT FINITE TEMPERATURES

The underlying equations of the QHD model can be derived from a field theory, starting from the semi-classical Hamiltonian which, in the absence of a magnetic field, reads [35, 46]

$$H[n(\mathbf{r}, t), w(\mathbf{r}, t)] = E[n(\mathbf{r}, t)] - \int eV_{\text{ext}}n(\mathbf{r}, t)d\mathbf{r} + \int \frac{m_e n(\mathbf{r}, t)}{2} |\nabla w(\mathbf{r}, t)|^2 d\mathbf{r} + \frac{e^2}{2} \int \frac{n(\mathbf{r}, t)n(\mathbf{r}', t)}{|\mathbf{r} - \mathbf{r}'|} d\mathbf{r}d\mathbf{r}', \quad (4)$$

where w is the scalar potential determining the velocity field by $\mathbf{v} = -\nabla w$, $E[n] = E_{\text{id}}[n] + E_{\text{xc}}[n]$ is the sum of the kinetic and the exchange-correlation energy functionals, and V_{ext} refers to the external electric potential.

Using $n(\mathbf{r}, t)$ and $m_e w(\mathbf{r}, t)$ as canonically conjugate field variables, we employ Hamilton's equations [49]:

$$\frac{\delta H[n(\mathbf{r}, t), w(\mathbf{r}, t)]}{m_e \delta w(\mathbf{r}, t)} = -\frac{\partial n(\mathbf{r}, t)}{\partial t}, \quad (5)$$

$$\frac{\delta H[n(\mathbf{r}, t), w(\mathbf{r}, t)]}{\delta n(\mathbf{r}, t)} = m_e \frac{\partial w(\mathbf{r}, t)}{\partial t}, \quad (6)$$

and obtain the following equations of motion that form the basis of QHD [46, 47]:

$$\frac{\partial}{\partial t} n(\mathbf{r}, t) = \nabla [n(\mathbf{r}, t) \nabla w(\mathbf{r}, t)], \quad (7)$$

$$m_e \frac{\partial}{\partial t} w(\mathbf{r}, t) = \frac{\delta E[n]}{\delta n} - eV_{\text{ext}} + e^2 \int \frac{n(\mathbf{r}', t)}{|\mathbf{r} - \mathbf{r}'|} d\mathbf{r}' + \frac{e^2}{2} m_e |\nabla w(\mathbf{r}, t)|^2. \quad (8)$$

Introducing the potential of the generalized force [48]

$$\mu[n(\mathbf{r}, t)] = \frac{\delta E[n(\mathbf{r}, t)]}{\delta n(\mathbf{r}, t)} + e\varphi(\mathbf{r}, t), \quad (9)$$

with the definition

$$\varphi(\mathbf{r}, t) = e \int \frac{n(\mathbf{r}', t)}{|\mathbf{r} - \mathbf{r}'|} d\mathbf{r}' - V_{\text{ext}}, \quad (10)$$

and making use of relations $\mathbf{v} = -\nabla w$ and $(\mathbf{v} \cdot \nabla)\mathbf{v} = \frac{1}{2}\nabla(\nabla w)^2$, we arrive at the QHD equation in terms of average density $n(\mathbf{r}, t)$, velocity $v(\mathbf{r}, t)$, and the generalized force $-\nabla\mu[\mathbf{r}, t]$ [46–48]

$$\frac{\partial}{\partial t} n(\mathbf{r}, t) + \nabla [n(\mathbf{r}, t) v(\mathbf{r}, t)] = 0, \quad (11)$$

$$m_e \frac{\partial}{\partial t} \mathbf{v}(\mathbf{r}, t) + m_e \mathbf{v}(\mathbf{r}, t) \nabla \mathbf{v}(\mathbf{r}, t) = -\nabla \mu(\mathbf{r}, t). \quad (12)$$

In previous works, Eq. (12) was obtained for the case of fully degenerate electrons (zero temperature limit). Equations (11) and (12) represent QHD equations in the micro-canonical ensemble, as they were derived from the semi-classical Hamiltonian (4) (alternatively, they can be obtained from a semi-classical Lagrangian [46]).

For the extension to finite temperature, we now switch to the grand canonical ensemble. There, these equations

have the same form, but n and w must be understood as quantities that are averaged over the grand ensemble [50, 51]. Now we generalize the momentum equation (12) to the finite temperature case where it is advantageous to use the free energy functional, $F[n]$, instead of $E[n]$. Indeed, in the grand canonical ensemble we have [51]

$$\frac{\delta E}{\delta n} = \frac{\delta \Omega}{\delta n}, \quad (13)$$

with the grand potential

$$\Omega[n(\mathbf{r})] = F[n(\mathbf{r})] - \mu_0 N, \quad (14)$$

where μ_0 is a constant defining the chemical potential of the system in thermodynamic equilibrium, and $N = \int n(\mathbf{r}) d\mathbf{r}$ corresponds to the mean value of the number of particles in the grand canonical ensemble. The derivation of Eq. (13) is given in the Appendix A.

It should be noted that, in Eq. (13), E is the average value of the energy over a grand canonical ensemble. With this, we obtain for the potential of the generalized force at finite temperature:

$$\mu[n(\mathbf{r}, t), T] + \mu_0 = \frac{\delta F[n(\mathbf{r}, t)]}{\delta n(\mathbf{r}, t)} + e\varphi(\mathbf{r}, t), \quad (15)$$

where $F[n] = F_{\text{id}}[n] + F_{\text{xc}}[n]$ is decomposed into the ideal (non-interacting) part $F_{\text{id}}[n]$, and the exchange correlation part $F_{\text{xc}}[n]$. In the static long wavelength limit (see below), the generalized force, $-\nabla\mu[n(\mathbf{r}, t), T]$, is related to the pressure P [52]

$$\nabla P = n \nabla \frac{\delta F[n(\mathbf{r}, t)]}{\delta n(\mathbf{r}, t)}, \quad (16)$$

which provides the link with the standard fluid theory, cf. Eq. (2).

III. DERIVATION OF THE BOHM POTENTIAL AND FERMI PRESSURE

A. General Expressions

In order to derive a potential related to the Fermi pressure and the Bohm potential, we neglect the exchange-correlation term, $F_{\text{xc}}[n]$, and turn to the local density approximation (LDA) with non-locality taken into account by the first order gradient correction to the noninteracting free energy functional [45, 53, 54]:

$$F_{\text{id}}[n] = F_0[n] + \int d\mathbf{r} a_2[n] |\nabla n(\mathbf{r})|^2, \quad (17)$$

where the free energy F_0 is defined via the free energy density

$$F_0[n] = \int f_0[n] d\mathbf{r}, \quad (18)$$

and the functional $a_2[n]$ still remains to be found. Substituting Eq. (17) into (15) we have:

$$\mu_{\text{id}}[n(\mathbf{r}, t), T] + \mu_0 = \frac{\partial f_0[n]}{\partial n} + \frac{\partial a_2[n]}{\partial n} |\nabla n(\mathbf{r})|^2 - 2\nabla [a_2[n] \nabla n(\mathbf{r})] + e\varphi(\mathbf{r}, t). \quad (19)$$

Now we show that it is possible to connect the QHD Bohm potential with the expansion of the inverse polarization function and, thereby, to obtain a_2 . For the static case, $\omega = 0$, this was done by Perrot [55]. Here we generalize his results to the dynamic case. We consider small localized variations of the potential, $\delta\varphi$, density, δn , velocity in terms of the scalar potential, δw , and of the chemical potential, $\delta\mu_{\text{id}}$. From Eq. (7), taking the equilibrium density distribution as uniform ($n_0 = \text{const}$) and assuming $w_0 = 0$, we obtain

$$\delta\tilde{w} = \frac{i\omega}{k^2 n_0} \delta\tilde{n}, \quad (20)$$

where $\delta\tilde{n}$, and $\delta\tilde{w}$ denote the Fourier transforms of δn and δw , respectively. The resulting variation of μ_{id} , as defined by Eq. (19), has the form [55]

$$\delta\mu_{\text{id}} = \left(\frac{\partial^2 f_0[n]}{\partial n^2} \Big|_{n=n_0} - 2a_2[n_0] \Delta \right) \delta n + e\delta\varphi. \quad (21)$$

Thus, the linearized momentum equation (12) for $\tilde{w} = \delta\tilde{w}$ and, taking into account Eq. (21), is written as:

$$-i\omega m_e \delta\tilde{w} = e\delta\tilde{\varphi} + \left[\frac{\partial^2 f_0[n]}{\partial n^2} \Big|_{n=n_0} + 2a_2[n_0] k^2 \right] \delta\tilde{n}. \quad (22)$$

Finally, making use of Eq. (20), we find

$$e\delta\tilde{\varphi} = - \left[\frac{\partial^2 f_0[n]}{\partial n^2} \Big|_{n=n_0} + 2a_2[n_0] k^2 - \frac{\omega^2 m_e}{k^2 n_0} \right] \delta\tilde{n}. \quad (23)$$

This is an important result that relates the density perturbation to the perturbation of the external potential. As we have assumed weak perturbations, we can make use of the results of linear response theory and identify in Eq. (23) the inverse polarization function, $\Pi^{-1} \equiv e\delta\tilde{\varphi}/\delta\tilde{n}$:

$$\frac{1}{\Pi(k, \omega)} = - \left[\frac{\partial^2 f_0[n]}{\partial n^2} \Big|_{n=n_0} + 2a_2[n_0] k^2 - \frac{\omega^2 m_e}{k^2 n_0} \right]. \quad (24)$$

B. RPA result for the Bohm potential and Fermi pressure

Equation (24) gives us the opportunity to express the r.h.s. of Eq. (24) systematically via linear response theory. The lowest order many-body approximation for Π is

the random phase approximation (RPA), which reads in equilibrium, for arbitrary temperature [56]

$$\Pi_{\text{RPA}}(k, \omega) = -\frac{k^2 \chi_0^2}{16\pi e^2 z^3} [g(u+z) - g(u-z)], \quad (25)$$

where we introduced dimensionless frequency and wave number, $u = \omega/(kv_F)$, $z = k/(2k_F)$, and defined $\chi_0^2 = (\pi k_F a_B)^{-1} \simeq r_s/6.03$, where a_B is the Bohr radius, $r_s \equiv a/a_B$, with a being the mean interparticle distance, and we also introduced the Fermi wave number and the plasma frequency, $k_F = (3\pi^2 n)^{1/3}$, $\omega_p^2 = 4\pi n e^2/m_e$. Finally, we defined

$$g(x) = -g(-x) = \int \frac{y dy}{\exp(y^2/\theta - \eta) + 1} \ln \left| \frac{x+y}{x-y} \right|. \quad (26)$$

With these explicit expressions the RPA polarization can be studied in detail. Particularly simple expressions exist for various limiting cases with respect to frequency and wave number. In the limiting cases of large or small values of z , the inverse of the real part of the RPA polarization function has the following expansion [56, 59]:

$$\frac{1}{2\Pi_{\text{RPA}}(z, u)} \simeq \tilde{a}_0 + \tilde{a}_2(2k_F)^2 z^2 + \tilde{a}_4(2k_F)^4 z^4 + \dots + cu^2 \\ \simeq \tilde{a}_0 + \tilde{a}_2 k^2 + \tilde{a}_4 k^4 + \dots + \frac{1}{2} \frac{\omega^2 m_e}{k^2 n_0}. \quad (27)$$

In particular, we obtain the long-wavelength limit of the inverse polarization function as

$$\frac{1}{\Pi^0(\omega)} \equiv \lim_{k \rightarrow 0} \frac{1}{\Pi_{\text{RPA}}(z, u)} = \frac{\omega^2 m_e}{k^2 n_0}. \quad (28)$$

Comparing Eqs. (24) and (27), we see that

$$\tilde{a}_0[n_0] = -\frac{1}{2} \frac{\partial^2 f_0[n]}{\partial n^2} \Big|_{n=n_0}, \quad (29)$$

$$\tilde{a}_2[n_0] = -a_2[n_0]. \quad (30)$$

The convergence of the expansion (27) is discussed in Appendix B for the static case and $k < 2k_F$.

We stress that the coefficients \tilde{a}_0 and a_2 depend on the considered limits for k and ω which directly affects the value of the Bohm potential, as will be shown below. Equations (29) and (30) are closely related to the *stiffness* theorem connecting the perturbation of an equilibrium state (of the energy, in the case of the ground state) due to an applied external field with an inverse linear response function. The proof of this theorem was given in Ref. [19] for the ground state and can be easily extended to finite temperatures.

Once the coefficients $\tilde{a}_0[n_0]$ and $a_2[n_0]$ are defined, we allow the equilibrium density to vary in space and time, $n_0 \rightarrow n(\mathbf{r}, t)$, according to the standard concept of LDA. The Bohm potential in the local density approximation, for QHD applications can be obtained for any degeneracy

parameter from the second term on the right hand side of Eq. (17):

$$V_B = \frac{\delta}{\delta n} \int d\mathbf{r} a_2[n] |\nabla n(\mathbf{r})|^2 \\ = |\nabla n|^2 \frac{\partial a_2[n]}{\partial n} - 2(a_2[n] \nabla^2 n + \nabla n \nabla a_2[n]). \quad (31)$$

The coefficients $\tilde{a}_0[n]$ and $a_2[n]$ are expressed in terms of the density $n(\mathbf{r})$ and the dimensionless chemical potential, $\eta = \beta\mu$, where we introduced the inverse temperature, $\beta = 1/(k_B T)$.

Using the local density approximation, we obtain $n(\mathbf{r}) = \frac{\sqrt{2m^{3/2}}}{\pi^2 \beta^{3/2} \hbar^3} I_{1/2}[\eta(\mathbf{r})]$. The following partial derivatives are needed to find the Bohm potential (31),

$$\frac{\partial \eta}{\partial n} = C \frac{1}{I_{-1/2}(\eta)}, \quad (32)$$

$$\nabla \eta = C \frac{\nabla n(\mathbf{r})}{I_{-1/2}(\eta)}, \quad (33)$$

where $C = \frac{2\pi^2 \beta^{3/2} \hbar^3}{\sqrt{2m^{3/2}}} = \frac{4}{3n} \theta^{-3/2}$. As is shown below, at $\theta = k_B T/E_F \sim T \times n^{-2/3} \rightarrow 0$, we have $a_2[n] = \gamma \hbar^2/(8mn)$, and the Bohm potential has the following form:

$$V_B(\omega, k) = \gamma(\omega, k) \frac{\hbar^2}{8m} \left(\left| \frac{\nabla n}{n} \right|^2 - 2 \frac{\nabla^2 n}{n} \right), \quad (34)$$

where the coefficient γ sensitively depends on the considered values of the wave number and frequency.

On the other hand, the Fermi pressure is proportional to the functional derivative of the Thomas-Fermi free energy [48], which, at $\theta \rightarrow 0$, can be written as:

$$\frac{\delta F_0[n]}{\delta n} = \frac{\partial f_0[n]}{\partial n} = - \int 2\tilde{a}_0([n], \theta \rightarrow 0) dn = \bar{\alpha} E_F, \quad (35)$$

where the coefficient $\bar{\alpha}$ depends on the considered limit on the k - ω plane. Previously, this coefficient was chosen by adjusting the QHD result for the longitudinal plasmon dispersion to the RPA prediction [43, 61] for zero temperature [note that $F \rightarrow E$, at $\theta \rightarrow 0$].

Now, we will use Eq. (29), to analyze different limits for the coefficients $\tilde{a}_0[n]$ and $a_2[n] = -\tilde{a}_2$, for different frequency-wavenumber ranges.

C. Low frequency and long wavelength limit, $\omega \ll \hbar k^2/2m, k \ll 2k_F$

The results given for the static case remain valid also for low frequencies, i.e. $u \ll 1$ or $\omega \ll kv_F$. This regime is relevant for a variety of physical processes such as the screening of a test charge and the dispersion of low-frequency waves (e.g. ion-acoustic waves) in a plasma. In

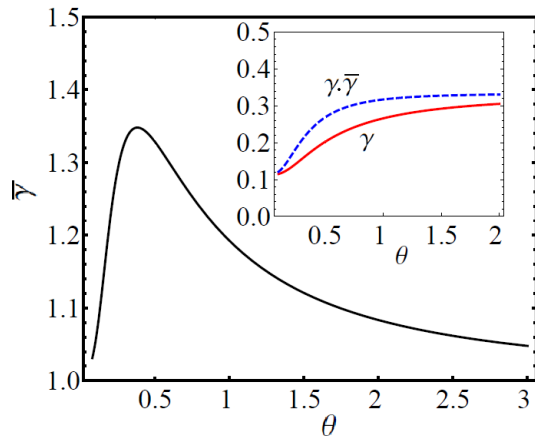


FIG. 1. The values of the factors $\bar{\gamma}$, γ , and $\gamma\bar{\gamma}$ in the finite temperature Bohm potential, Eq. (47), for the long-wavelength case.

a variety of publications e.g. the topic of screening of an ion in a quantum plasma were treated incorrectly using the Bohm potential for the high-frequency case rather than for the static case. This has led to the unphysical prediction of ion-ion attraction in an equilibrium quantum plasma, for a discussion, see Refs. [40, 45]. To obtain the Fermi pressure and Bohm potential in the present limiting case, we calculate the coefficients $\tilde{a}_0[n]$ and $a_2[n]$ and obtain [45]:

$$\tilde{a}_0[n] = -\frac{\pi e^2}{2k_F^2 \chi_0^2 H_1(\eta)}, \quad (36)$$

$$a_2[n] = -\frac{\hbar^2 H_2(\eta)}{72m_e n H_1^2(\eta)}, \quad (37)$$

with

$$H_1(\eta) = \frac{\sqrt{\theta[n]}}{2} I_{-1/2}(\eta), \quad H_2(\eta) = \frac{1}{2\sqrt{\theta[n]}} I_{-3/2}(\eta).$$

In the low-temperature limit, $\theta \rightarrow 0$, we have $H_1(\eta) \simeq 1$ and $H_2 \simeq -1$, and Eq. (37) gives the asymptotic results $a_2 \rightarrow \hbar^2/(72mn)$ and $\gamma = 1/9$ for the coefficient in front of the Bohm potential in Eq. (34) [45, 55, 57, 58].

Using the relations (32) and (33), the finite-temperature generalization of the Bohm potential can be easily found by substituting Eq. (37) into Eq. (31) and taking into account the dependence $\theta[n] \sim n^{-2/3}$. Furthermore, for the static case ($\omega = 0$), we have $f_0 \equiv f_{\text{TF}}$, where f_{TF} is the Thomas-Fermi free energy density:

$$f_{\text{TF}}([n], \theta) = \frac{\sqrt{2}m^{3/2}}{\hbar^3 \pi^2 \beta^{5/2}} \left(\eta I_{1/2}(\eta) - \frac{2}{3} I_{3/2}(\eta) \right), \quad (38)$$

where I_ν is the Fermi integral of order ν . Using Eq. (38) Perrot [55] showed that the second order partial derivative of the Thomas-Fermi density of states, $-\frac{1}{2} \frac{\partial^2 f_{\text{TF}}[n]}{\partial n^2}$, in the static long wave length limit ($k \ll 2k_F$) exactly coincides with $\tilde{a}_0[n]$ given by Eq. (36). Finally, the func-

tional derivative of the Thomas-Fermi term yields:

$$\frac{\delta F_{\text{TF}}}{\delta n} = \frac{\eta}{\beta}. \quad (39)$$

At zero temperature, $\eta = \beta E_F$, leading to $\delta T_{\text{TF}}/\delta n = E_F$, in agreement with the result of Ref. [48].

By regrouping terms we can rewrite the Bohm potential (31) in the following form:

$$V_B = V_1 + V_2, \quad (40)$$

where

$$V_1 = -2a_2[n] \nabla^2 n, \quad (41)$$

and

$$\begin{aligned} V_2 &= |\nabla n|^2 \frac{\partial a_2[n]}{\partial n} - 2\nabla n \frac{\partial a_2[n]}{\partial r} \\ &= |\nabla n|^2 \frac{\partial \eta}{\partial n} \frac{\partial a_2[n]}{\partial \eta} - 2\nabla n \frac{\partial \eta}{\partial r} \frac{\partial a_2[n]}{\partial \eta} \\ &= -|\nabla n|^2 \frac{C}{I_{-1/2}(\eta)} \frac{\partial a_2[n]}{\partial \eta}, \end{aligned} \quad (42)$$

and the last line of Eq. (42) was obtained using relations (32) and (33). In order to analyze finite temperature effects we introduce the coefficient:

$$\gamma[n] = a_2[n] \left(\frac{\hbar^2}{8m_e n} \right)^{-1} = -\frac{2}{9} \frac{I_{-3/2}(\eta)}{I_{-1/2}^2(\eta)} \theta^{-3/2}, \quad (43)$$

similar to the zero-temperature case, and use it in V_1 to obtain

$$V_1 = \gamma \frac{\hbar^2}{8m_e} \left(-2 \frac{\nabla^2 n}{n} \right). \quad (44)$$

By taking into account that $C = \frac{4}{3n} \theta^{-3/2}$, we find:

$$V_2 = -\gamma \frac{\hbar^2}{8m_e} \frac{2I_{-1/2}(\eta)I_{1/2}(\eta)}{I_{-3/2}(\eta)} \frac{\partial a_2[n]}{\partial \eta} \times \frac{|\nabla n|^2}{n^2}. \quad (45)$$

Finally, we introduce the coefficient:

$$\bar{\gamma}[n] = -\frac{2I_{1/2}(\eta)I_{-1/2}(\eta)}{I_{-3/2}(\eta)} \frac{\partial}{\partial \eta} \left(\frac{I_{-3/2}(\eta)}{I_{-1/2}^2(\eta)} \right), \quad (46)$$

and substitute Eqs. (44) and (45) into Eq. (40). This yields the following expression for the finite-temperature Bohm potential in the static long wavelength limit:

$$V_B(\theta) = \gamma(\theta) \frac{\hbar^2}{8m} \left(\bar{\gamma}(\theta) \left| \frac{\nabla n}{n} \right|^2 - 2 \frac{\nabla^2 n}{n} \right). \quad (47)$$

The correction coefficient $\bar{\gamma}$ of the first term in the Bohm potential for the finite-temperature case (47), and the dependence of γ and $\gamma\bar{\gamma}$ on θ are presented in Fig. 1. In the limit of fully degenerate electrons, $\theta \rightarrow 0$, as well

as in the classical limit, $\theta \gg 1$, the correction coefficient approaches unity, $\bar{\gamma} \rightarrow 1$. This correction coefficient $\bar{\gamma}$ is important for a partially degenerate plasma, around $\theta \sim 0.5$, as can be seen from Fig. 1.

Recently, Haas and Mahmood [60] considered the finite-temperature Bohm potential by analyzing ion-acoustic waves on the basis of linearized QHD equations and comparing them with the RPA result. They correctly derived the coefficient γ in Eq. (43), but missed the correction coefficient $\bar{\gamma}$ in Eq. (46). Note that in Eq. (47), the second term of the Bohm potential is proportional to n_1/n_0 , whereas the first term $\sim (n_0/n_1)^2$, where n_1 is a small density perturbation (i.e., $n_0/n_1 \ll 1$). As a result, in the linear approximation, which was considered by Haas and Mahmood [60], the information about the first term of the Bohm potential and the coefficient $\bar{\gamma}$ is lost.

D. Short wavelength limit, $k \gg 2k_F$ at low frequencies, $\omega \ll \hbar k^2/2m$

For the degenerate electron gas, Jones and Yang [61] showed that, in the short wavelength limit, the first order gradient correction term of the non-interacting kinetic energy has the form of the von Weizsäcker gradient correction with $a_2[n] = \frac{\hbar^2}{8m_e n}$, which gives $\gamma = 1$ for the Bohm potential. This result is important as the von Weizsäcker gradient correction correctly reproduces Kato's cusp condition for the electron distribution close to a test charge (core) [63]. Knowledge of the change of the coefficients determining the Fermi pressure and Bohm potential at the transition from the long wavelength limit to the short wavelength case can be useful to analyze the QHD results in plasmonics [10, 65], quantum plasmas [64] and the application of orbital-free DFT to dense plasmas (warm dense matter) [2, 66, 72].

In the low-frequency short wavelength limit, $u \ll z$, $z \gg 1$, we use the following expansion of the function $\Delta g = g(u+z) - g(u-z)$ [56]:

$$\Delta g \simeq 2g(z) + u^2 g''(z), \quad (48)$$

where

$$g(z) = \frac{2}{3z} + \frac{I_{3/2}\theta^{5/2}}{3z^3}. \quad (49)$$

From Eqs. (48) and (49) we obtain

$$\frac{z}{\Delta g} \simeq -\frac{3}{8}I_{3/2}(\eta)\theta^{5/2} + \frac{3z^2}{4} - \frac{3u^2}{4} + \dots, \quad (50)$$

which can be substituted into the formula for the inverse polarization function, with the result

$$\frac{1}{\Pi(k, \omega)} = -\frac{4\pi e^2}{\chi_0^2 k_F^2} \frac{z}{\Delta g}. \quad (51)$$

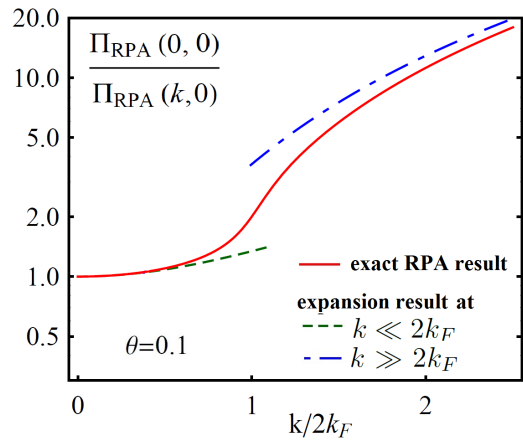


FIG. 2. The values of the quantity $\Pi_{\text{RPA}}(0,0)/\Pi_{\text{RPA}}(k,0)$ at $\theta = 0.1$.

From this, we obtain the coefficients $\tilde{a}_0[n]$ and $a_2[n]$ in the short wavelength case:

$$\tilde{a}_0[n] = -\frac{4\pi e^2}{k_F^2 \chi_0^2} \times \frac{3}{16} I_{3/2}(\eta) \theta^{5/2} [n], \quad (52)$$

$$a_2[n] = \frac{\hbar^2}{8m_e n}. \quad (53)$$

From Eq. (53) we see that the coefficient in front of the Bohm potential in Eq. (34) becomes $\gamma = 1$ [61], and it is interesting to note that, in the short wavelength limit, the Bohm potential is independent of temperature. Consider now the Fermi pressure term. At small temperatures, $\theta \ll 1$, using Eq. (52) for the functional derivative of $F_0[n]$ yields

$$\frac{\delta F_0[n]}{\delta n} = \frac{3}{5} E_F + \frac{3\pi^2}{8} E_F \theta^2, \quad (54)$$

where the first term is the result for the ground state and the second term is the finite-temperature correction. Thereby, the transition from the long wavelength to the short wavelength limit leads to a change of the factor $\bar{\alpha}$, from 1 to 3/5. Note that, in the short wavelength limit, or for large values of the density gradient the von Weizsäcker gradient correction is the leading term in the non-interacting free energy functional of electrons [63].

In Fig. 2 the results of the expansions of the inverse RPA polarization function in the limits of long, $k/2k_F \ll 1$, and short wavelengths, $k/2k_F \gg 1$, are compared with the exact RPA result. It can be concluded that, in the case of the uniform electron gas, the long-wavelength limit result is applicable up to $k \simeq k_F$.

E. High frequency limit, $\omega \gg \hbar k^2/2m$

The present limiting case is important for a variety of physical situations, such as for the description of the

optical (Lengmuir) plasmon of the electrons as well as for the plasma response to a high-frequency electromagnetic field with frequencies exceeding the plasma frequency.

To obtain the correct pre-factors of the Bohm potential and Fermi pressure in the present high-frequency limit, $u \gg z$, we use the formulas [56]

$$g(u+z) - g(u-z) = 2zg'(u) + \frac{z^3}{3}g'''(u), \quad (55)$$

$$g(u) = \frac{2}{3u} + \frac{I_{3/2}\theta^{5/2}}{3u^3}, \quad (56)$$

and obtain

$$\frac{z}{\Delta g} \simeq -\frac{9}{8}I_{3/2}(\eta)\theta^{5/2} + \frac{3z^2}{4} - \frac{3u^2}{4} + \dots \quad (57)$$

The coefficients $\tilde{a}_0[n]$ and $a_2[n]$ are obtained from Eqs. (57) and (51)

$$\tilde{a}_0[n] = -\frac{4\pi e^2}{k_F^2 \chi_0^2} \times \frac{9}{16}I_{3/2}(\eta)\theta^{5/2}[n], \quad (58)$$

$$a_2[n] = \frac{\hbar^2}{8m_e n}. \quad (59)$$

Equation (59) shows that the coefficient in front of the Bohm potential equals $\gamma = 1$. In the high-frequency limit the coefficient $a_2[n]$ does not depend on temperature, which means that at finite temperature the Bohm potential is given by Eq. (34). This is explained by the fact that, at sufficiently high frequency of the perturbing electric field, the back and forth movement of the electrons is not affected by their thermal motion.

From Eq. (58), the high-frequency analogue of the Thomas-Fermi pressure can be obtained using $-\int 2\tilde{a}_0[n]dn$. In the zero-temperature limit, taking into account the relation $I_{3/2}(\theta \rightarrow 0) = \frac{2}{5}\theta^{-5/2}$ leads to the following expression for the functional derivative of $F_0[n]$, at high frequency:

$$\frac{\delta F_0[n]}{\delta n} = \frac{9}{5}E_F. \quad (60)$$

Equation (60) indicates that, in the high-frequency limit, the QHD equations contain the coefficient $\bar{\alpha} = 9/5$. We note that, in previous works [35, 43], this constant coefficient was artificially added in order to reach agreement between the results of the QHD and the RPA expression for the plasmon dispersion relation.

A finite-temperature correction to Eq. (60) can be obtained by expanding $I_{3/2}(\eta)$ around $\theta = 0$,

$$\frac{\delta F_0[n]}{\delta n} = \frac{9}{5}E_F + \frac{9\pi^2}{8}E_F\theta^2. \quad (61)$$

The different values of the factors γ and $\bar{\alpha}$ in the k - ω plane are summarized in Fig. 3. Furthermore, the information about the obtained coefficients $a_2[n]$, γ and $\tilde{a}_0[n]$, $\bar{\alpha}$ is listed in tables I and II.

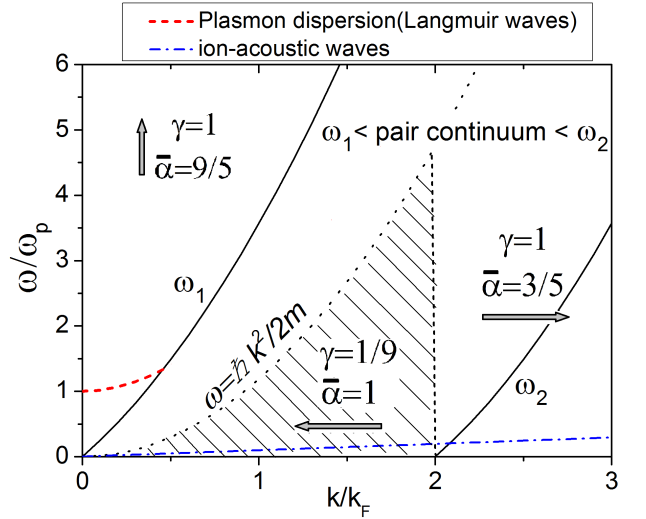


FIG. 3. The values of the factors γ in Bohm potential Eq.(34) and $\bar{\alpha}$ in Eq.(35) for different cases on (k, ω) plane at $\theta \ll 1$. The area between curves ω_1 and ω_2 corresponds to the pair continuum. Dashed line is the plasmon dispersion $\omega = \omega_p^2 + (3/5)k^2v_F^2 + (1/4)\hbar^2k^4/m_e^2$ and dash-dot line is frequency of the ion-acoustic waves multiplied by m_p/m_e . Dashed area corresponds to the static long wave length limit. Arrows indicate that the factors γ and $\bar{\alpha}$ were obtained for different limits (see Tables II and I).

TABLE I. The prefactor of the Bohm potential γ [cf. Eq. (47)] and the expansion coefficient $a_2[n]$ in different limits

	$a_2[n]$	γ
$\omega \ll \hbar k^2/2m_e$ $k \ll 2k_F$	$-\frac{\hbar^2 H_2(\eta)}{72m_e n H_1^2(\eta)}$	1/9
$\omega \ll \hbar k^2/2m_e$ $k \gg 2k_F$	$\frac{\hbar^2}{8m_e n}$	1
$\omega \gg \frac{\hbar k^2}{2m_e}$	$\frac{\hbar^2}{8m_e n}$	1

Using the high-frequency result for \tilde{a}_0 and the Bohm potential, one can derive the well-known plasmon dispersion from the continuity and momentum equations:

$$\omega^2(k) = \omega_p^2 - 2\tilde{a}_0[n_0]\frac{n_0}{m_e} \times k^2 + \frac{\hbar^2 k^4}{4m_e^2}, \quad (62)$$

which, at $\theta \ll 1$, approaches the form

$$\omega^2(k) = \omega_p^2 + \frac{3}{5}v_F^2 k^2 + \frac{\hbar^2 k^4}{4m_e^2}, \quad (63)$$

where we took into account that $2\tilde{a}_0[n_0]n_0/m_e \rightarrow -\frac{3}{5}v_F^2$, at $\theta \rightarrow 0$, and that, in the high-frequency limit, $a_2[n] = \hbar^2/8m_e n$.

On the other hand, in the limit $\theta \gg 1$, taking into account that $\tilde{a}_0[n_0] \rightarrow -\frac{3}{2}\frac{k_B T}{n_0}$, leads to the dispersion

TABLE II. The prefactor $\bar{\alpha}$ of the Fermi pressure [cf. Eq. (35)] and the expansion coefficient $\tilde{a}_0[n]$ in different limits.

	$\tilde{a}_0[n]$	$\bar{\alpha}$
$\omega \ll \frac{\hbar k^2}{2m_e}$ $k \ll 2k_F$	$-\frac{\pi e^2}{2k_F^2 \chi_0^2 H_1(\eta)}$	1
$\omega \ll \frac{\hbar k^2}{2m_e}$ $k \gg 2k_F$	$-\frac{4\pi e^2}{k_F^2 \chi_0^2} \times \frac{3}{16} I_{3/2}(\eta) \theta^{5/2}$	$\frac{3}{5}$
$\omega \gg \frac{\hbar k^2}{2m_e}$	$-\frac{4\pi e^2}{k_F^2 \chi_0^2} \times \frac{9}{16} I_{3/2}(\eta) \theta^{5/2}$	$\frac{9}{5}$

relation

$$\omega^2(k) = \omega_p^2 + 3v_{\text{th}}^2 k^2 + \frac{\hbar^2 k^4}{4m_e^2}, \quad (64)$$

where $v_{\text{th}} = \sqrt{\frac{k_B T}{m_e}}$ is the thermal velocity of the electrons.

Note that the linearized QHD equations correctly reproduce the dynamic RPA polarization function in the long wavelength limit, $\Pi^0(\omega)$, Eq. (28), without any additional terms related to the fermionic pressure.

IV. GENERALIZED NON-LOCAL BOHM POTENTIAL IN LINEAR RESPONSE

In the previous section, the Bohm potential of quantum hydrodynamics was derived on the basis of the RPA polarization function, using the expansion of the latter in powers of the wavenumber. This has allowed us to improve the QHD model, depending on the wavenumber and frequency range in three relevant cases, by involving the dynamic LDA and the gradient correction, on the basis of the RPA

On the other hand, QHD can be used to independently obtain the response function of (uncorrelated) electrons, $\Pi_{\text{QHD}}^{\text{id}}(k, \omega)$, for arbitrary frequencies and wavenumbers. In particular, at large wavenumbers the previous power expansion is not applicable. It is, therefore, instructive to inquire whether this expansion can be entirely avoided. The idea is again to enforce agreement with the polarization function of linear response theory, but now in the whole frequency-wavenumber range. The simplest solution is, again, to use the full (non-local) RPA polarization and to require

$$\Pi_{\text{QHD}}^{\text{id}}(k, \omega) \equiv \Pi_{\text{RPA}}(k, \omega). \quad (65)$$

This will result in a generalized non-local Bohm potential.

We now derive a relation between the free energy of the system and the RPA polarization. To this end, we consider an equilibrium density profile $n_0(\mathbf{r})$ that is current-

free, $w_0(\mathbf{r}) = 0$ and which follows, as before, from

$$\frac{\delta F[n_0(\mathbf{r})]}{\delta n_0(\mathbf{r})} + e\varphi_0(\mathbf{r}) = \mu_0, \quad (66)$$

where μ_0 is a constant. The equilibrium configuration is now exposed to a weak external perturbation giving rise to $n(\mathbf{r}, t) = n_0(\mathbf{r}) + n_1(\mathbf{r}, t)$, $w(\mathbf{r}, t) = w_1(\mathbf{r}, t)$, $\varphi(\mathbf{r}, t) = \varphi_0(\mathbf{r}) + \varphi_1(\mathbf{r}, t)$. The first order perturbations follow by taking the continuity equation in first order in the perturbations,

$$\frac{\partial n_1(\mathbf{r}, t)}{\partial t} - \nabla \cdot (n_0 \nabla w_1) = 0, \quad (67)$$

and, similarly, the momentum equation [46]

$$m_e \frac{\partial w_1(\mathbf{r}, t)}{\partial t} = e\varphi_1(\mathbf{r}, t) + \int d\mathbf{r}' \frac{\delta^2 F[n]}{\delta n(\mathbf{r}, t) \delta n(\mathbf{r}', t)} \Big|_{n=n_0} n_1(\mathbf{r}', t), \quad (68)$$

where w_1 determines the velocity perturbation via $\mathbf{v}_1 = -\nabla w_1$, and the last term on the right hand side of Eq. (68) represents the total potential of the fermionic pressure which includes the Fermi pressure, Bohm potential and, in general, the exchange-correlation terms.

Now we again assume the equilibrium density to be uniform and consider small fluctuating quantities n_1 , w_1 . From Eqs. (67) and (68) we obtain, after Fourier transform to frequency and wavenumber (k, ω) space, which we denote by \mathfrak{F}

$$-i\omega \tilde{n}_1 + k^2 n_0 \tilde{w}_1 = 0, \quad (69)$$

$$-i\omega \tilde{w}_1 = \frac{e\tilde{\varphi}_1}{m_e} + \mathfrak{F} \left[\frac{\delta^2 F[n]}{\delta n(\mathbf{r}, t) \delta n(\mathbf{r}', t)} \Big|_{n=n_0} \right] \frac{\tilde{n}_1}{m_e}, \quad (70)$$

From Eqs. (69) and (70), immediately follows the QHD result for the inverse polarization function $\Pi_{\text{QHD}}^{-1}(k, \omega) = e\tilde{\varphi}_1/\tilde{n}_1$:

$$\Pi_{\text{QHD}}^{\text{id}-1}(k, \omega) = \frac{m_e \omega^2}{n_0 k^2} - \mathfrak{F} \left[\frac{\delta^2 F[n]}{\delta n(\mathbf{r}) \delta n(\mathbf{r}') } \Big|_{n=n_0} \right]. \quad (71)$$

Neglecting the exchange-correlation contribution to the free energy and taking $\Pi_{\text{QHD}} = \Pi_{\text{RPA}}$, it is straightforward to deduce from Eq. (71) that:

$$- \mathfrak{F} \left[\frac{\delta^2 F_{\text{id}}}{\delta n(\mathbf{r}, t) \delta n(\mathbf{r}', t)} \Big|_{n=n_0} \right] = \frac{1}{\Pi_{\text{RPA}}(k, \omega)} - \frac{1}{\Pi^0(\omega)}, \quad (72)$$

where we used the definition (28) of the long-wavelength limit, $\Pi^0(\omega)$, of the RPA polarization. As it was mentioned previously, Eq. (72) incorporates both the Fermi and Bohm potentials. In QHD, Eq. (72) can be used without additional separation of different contributions.

Now we verify that the generalized result, Eq. (72), correctly reproduces the results for the Bohm potential for the special cases that were obtained in the previous section. We do not use the (ideal) free energy density in the form of a gradient expansion, Eq. (17), but, instead, start from the more general non-local form [21, 45]:

$$F_{\text{id}}[n] = F_0[n_0(\mathbf{r})] + \int d\mathbf{r} d\mathbf{r}' K([n_0]; |\mathbf{r} - \mathbf{r}'|) n_1(\mathbf{r}, t) n_1(\mathbf{r}', t), \quad (73)$$

where the kernel K is symmetric with respect to permutation of \mathbf{r} and \mathbf{r}' . Using Eqs. (18) and (29), Eq. (73) can

be written as:

$$\mathfrak{F} \left[\frac{\delta^2 F_{\text{id}}}{\delta n(\mathbf{r}, t) \delta n(\mathbf{r}', t)} \Big|_{n=n_0} \right] = -2\tilde{a}_0[n_0] + 2\tilde{K}(\mathbf{k}). \quad (74)$$

where $\tilde{K}([n]; \mathbf{k})$ is the Fourier transform of the kernel K . Substituting Eq. (74) into Eq. (72) we find for K , after the inverse Fourier transformation,

$$K([n_0]; |\mathbf{r} - \mathbf{r}'|) = \mathfrak{F}^{-1} \left[-\frac{1}{2\Pi_{\text{RPA}}(k, \omega)} + \frac{1}{2\Pi^0(\omega)} + \tilde{a}_0[n_0] \right], \quad (75)$$

and, for the generalized non-local Bohm potential, we have

$$V_B[n(\mathbf{r}, t)] = \int 2K([n_0]; |\mathbf{r} - \mathbf{r}'|) n_1(\mathbf{r}') d\mathbf{r}' + \int \frac{\partial K([n_0], |\mathbf{r} - \mathbf{r}'|)}{\partial n} n_1(\mathbf{r}) n_1(\mathbf{r}') d\mathbf{r}' - \nabla \int \frac{\partial}{\partial \nabla n} \left(K([n_0], |\mathbf{r} - \mathbf{r}'|) n_1(\mathbf{r}) n_1(\mathbf{r}') \right) d\mathbf{r}' = \int 2K([n_0]; |\mathbf{r} - \mathbf{r}'|) n_1(\mathbf{r}') d\mathbf{r}' + \mathcal{O}\left(\frac{n_1}{n_0}\right)^2, \quad (76)$$

where we have used the abbreviation $n_1(\mathbf{r}) = n_1(\mathbf{r}, t)$.

Utilizing the expansion (27) we arrive at

$$\tilde{K}([n_0]; \mathbf{k}) = \tilde{a}_2[n_0] k^2 + \tilde{a}_4[n_0] k^4 + \dots, \quad (77)$$

and obtain, after inverse Fourier transformation

$$K([n_0]; |\mathbf{r} - \mathbf{r}'|) = a_2[n_0] \nabla \nabla' \delta(\mathbf{r} - \mathbf{r}') + a_4[n_0] \nabla^2 \nabla'^2 \delta(\mathbf{r} - \mathbf{r}') + \dots \quad (78)$$

Considering only the first term on the right-hand-side of Eq. (78), one can find the Bohm potential from (76) in the form of Eq. (31). Furthermore, higher order terms give rise to higher order gradient corrections to the non-interacting free energy density functional [45, 67–70]. For more details on the convergence of the gradient expansion in the ground state, we refer the reader to Ref. [71] and the references therein.

The closure relation Eq. (72) for the QHD equations (11) and (12) provides a unified general picture for the understanding of the complex parametric dependencies of the pre-factors of both Fermi pressure and Bohm potential on frequency, wavenumber, density and temperature. Moreover, it indicates ways how to systematically go beyond both the local density approximation and the model of an ideal Fermi gas. The inclusion of exchange and correlation effects will be performed in Sec. V whereas further issues of non-locality will be discussed in Sec. VI.

On the other hand, the local version of QHD, i.e. LDA with first order density gradient corrections, has now also

been clarified. Indeed, there is no inconsistency in using one set of pre-factors in front of the Bohm potential and Fermi pressure for computing the equilibrium (static) density profile and another one for the study of the time-dependent perturbation around the equilibrium equilibrium state. But within this approach, one can use more sophisticated free energy density functionals that were recently developed in orbital-free DFT [72, 73, 81] for the calculation of the equilibrium density distribution, taking into account correlation effects. As the next step one can use the general expression (72) or the approximation discussed in Sec. III.E for the consideration of the time-dependent density perturbation. The only question remaining is how to include in the most consistent way correlation effects into the QHD description of the density perturbation of arbitrary frequency. This question is discussed in the following section.

V. EXCHANGE-CORRELATION POTENTIAL FOR QHD APPLICATION

Now we make progress in another direction: we include, in addition to the ideal free energy, also the exchange-correlation free energy functional F_{xc} . This will allow us to generalize the polarization function from the ideal to the interacting case, $\Pi_{\text{QHD}}^{\text{id}} \rightarrow \Pi_{\text{QHD}}$. We note that for $T = 0$ exchange correlation contributions were included in QHD phenomenologically in Ref. [42].

A. QHD and local field corrections

It is known from linear response theory and DFT that the exchange-correlation free energy can be obtained from the local field correction [73, 74]. Now we use the same approach to derive the exchange-correlation potential for the QHD application.

Taking into account the result from Eq. (72) for the second order functional derivative of $F_{\text{id}}[n]$, we find from Eq. (71):

$$\Pi_{\text{QHD}}(k, \omega) = \frac{\Pi_{\text{RPA}}(k, \omega)}{1 - \mathfrak{F} \left[\left. \frac{\delta^2 F_{\text{xc}}}{\delta n(\mathbf{r}) \delta n(\mathbf{r}')} \right|_{n=n_0} \right] \Pi_{\text{RPA}}(k, \omega)}. \quad (79)$$

Interestingly, this expression has the same form as the density response function of a correlated electron gas, e.g. [75] or the polarization function, within the formalism of local field corrections [74]:

$$\Pi_{\text{LFC}}(k, \omega) = \frac{\Pi_{\text{RPA}}(k, \omega)}{1 + \tilde{u}(k)G(k, \omega)\Pi_{\text{RPA}}(k, \omega)}, \quad (80)$$

with $\tilde{u}(k) = 4\pi e^2/k^2$ being the Fourier transform of the Coulomb potential. From the requirement that the correlated QHD polarization is in agreement with the latter result, i.e. $\Pi_{\text{QHD}}(k, \omega) \equiv \Pi_{\text{LFC}}(k, \omega)$, we now have the possibility to derive the exchange-correlation free energy in terms of local field corrections, for application in the QHD equation (68):

$$\mathfrak{F} \left[\left. \frac{\delta^2 F_{\text{xc}}}{\delta n(\mathbf{r}) \delta n(\mathbf{r}')} \right|_{n=n_0} \right] = -\tilde{u}(k)G(k, \omega). \quad (81)$$

Note that a similar result was obtained in the framework of TDDFT [19, 23]. The analytic properties of the dynamic local field correction, such as the asymptotic expansion, were studied in detail by Kugler [76]. The interpolation formula for the dynamic local field correction was considered in Refs. [77] and [78].

The static local field correction $G(k)$ can be obtained using the finite temperature STLS approximation [79–81] or by *ab initio* quantum Monte Carlo simulations [4]. In the latter case, $G(k)$ can be represented by a fit formula for small and large wave numbers [82, 83], $G(k) = A[1 - \exp(-Bk^2)]$, where the coefficients A and B can be obtained using analytical fits for the exchange-correlation free energy per electron, f_{xc} , and the pair-distribution function of the uniform electron gas, $g(r)$, at $r \rightarrow 0$, based on quantum Monte Carlo data [73]. For the ground state, $\theta \rightarrow 0$, an accurate analytical formula of $G(k)$ which has been fitted to quantum Monte Carlo data [84] was presented by M. Corradini *et al.* [85]. For the finite temperature case, an accurate parametrization of the exchange-correlation free energy has been provided recently by Groth *et al.* [86], and first *ab initio* calculations of the local field correction were presented in Ref. [88].

Further, knowing the static local field correction, the dynamic result for $G(k, \omega)$ can be calculated, for instance, on the basis of the method of moments [90]. Alternatively, the dynamic STLS approximation can be used to calculate $G(k, \omega)$ for both ground state [91] and at finite temperature [92, 93].

B. Collision effects in relaxation-time approximation

In order to illustrate the effect of correlations in the most simple way, let us consider the polarization function in the relaxation time approximation (Mermin polarization function) [54, 94]:

$$\Pi_{\text{LFC}}(k, \omega) = \frac{\Pi_{\text{RPA}}(k, \omega)}{1 + i\hbar\nu\tilde{\Pi}(k, \omega)}, \quad (82)$$

with the definition

$$\tilde{\Pi}(k, \omega) = \frac{1}{\hbar\omega} \left[\frac{\Pi_{\text{RPA}}(k, \omega)}{\Pi_{\text{RPA}}(k, 0)} - 1 \right], \quad (83)$$

and ν being the electron collision frequency. Comparison of Eqs. (80) and (82), leads to:

$$\frac{4\pi e^2}{k^2}G(k, \omega) = \frac{i\nu}{\omega} \left[\frac{1}{\Pi_{\text{RPA}}(k, 0)} - \frac{1}{\Pi_{\text{RPA}}(k, \omega)} \right]. \quad (84)$$

In the long-wavelength limit, $k \rightarrow 0$, we use the expansion (27), and derive from Eq. (84)

$$\begin{aligned} \frac{4\pi e^2}{k^2}G(k, \omega) &\simeq \frac{i\nu}{\omega} \left[2\left(\tilde{a}_0^0[n_0] - \tilde{a}_0[n_0]\right) + \right. \\ &\quad \left. 2\left(\tilde{a}_2^0[n_0] - \tilde{a}_2[n_0]\right)k^2 - \frac{1}{\Pi^0(\omega)} \right] \\ &\simeq -\frac{im_e \omega \nu}{n_0 k^2}, \end{aligned} \quad (85)$$

where $\tilde{a}_0[n_0]$ and $\tilde{a}_2[n_0]$, are the (frequency-dependent) expansion coefficients of the RPA polarization in the long-wavelength limit that were given in tables I and II, and $\tilde{a}_0^0[n_0]$ and $\tilde{a}_2^0[n_0]$ are the respective zero-frequency limits.

For the exchange-correlation term in the momentum equation (70), the relaxation time approximation gives rise to a friction force:

$$\begin{aligned} \int d\mathbf{r}' \left. \frac{\delta^2 F_{\text{xc}}[n]}{\delta n(\mathbf{r}, t) \delta n(\mathbf{r}', t)} \right|_{n=n_0} n_1(\mathbf{r}', t) = \\ \mathfrak{F}^{-1} \left[-\frac{4\pi e^2}{k^2}G(k, \omega)\tilde{n}_1 \right] = \mathfrak{F}^{-1} \left[\frac{im_e \omega \nu}{n_0 k^2}\tilde{n}_1 \right] = \\ \mathfrak{F}^{-1} [\nu\tilde{w}_1 m_e] = \nu w_1(\mathbf{r}, t) m_e, \end{aligned} \quad (86)$$

where $\tilde{w}_1 = \frac{i\omega}{k^2 n_0}\tilde{n}_1$, and Eqs. (81) and (85) were used. If one retains also terms scaling as $\sim \tilde{a}_0$, and $\sim \tilde{a}_2$ in Eq. (85), the so-called hydrodynamic Drude model used in plasmonics [35, 43, 95] is recovered.

This example corresponds to the simplest form of the dynamic exchange-correlation potential. However, this approximation appears to be very useful for the description of dense plasmas and warm dense matter if one extends the model to a dynamic collision frequency,

$\nu = \nu(\omega)$ [96–99]. In this case, $\nu(\omega)$ can be computed taking into account quantum and non-ideality effects by other techniques such as quantum kinetic theory or Green functions [96], or semiclassical molecular dynamics simulations [100].

Now we can write down the general form of the QHD momentum equation:

$$m_e \frac{\partial w_1(\mathbf{r}, t)}{\partial t} = e\varphi_1(\mathbf{r}, t) + \int d\mathbf{r}' n_1(\mathbf{r}', t) \left[\int d\mathbf{k} d\omega e^{i[\mathbf{k}\cdot(\mathbf{r}-\mathbf{r}')-i\omega t]} \left(-\frac{1}{\Pi_{\text{RPA}}(k, \omega)} + \frac{1}{\Pi^0(\omega)} - \frac{4\pi e^2}{k^2} G(k, \omega) \right) \right] \Big|_{n_0 \rightarrow n_0(\mathbf{r}')} , \quad (87)$$

where the notation $n_0 \rightarrow n_0(\mathbf{r})$ emphasizes that the initially constant equilibrium density is allowed to vary in space, but only after performing the inverse Fourier transformation to real space.

VI. SUMMARY

In this paper, first of all, previously known results on QHD have been revisited and extended. To this end we started with a general expression for the free energy as a functional of the density and used the local density approximation together with gradient corrections. Explicit results were obtained in different limiting cases and compared to the RPA polarization function. The factors $\bar{\alpha}$ and γ in the equation for the Fermi pressure and the Bohm potential have been derived consistently connecting the linear density response function in the RPA to the Thomas-Fermi theory complemented by the first order density gradient correction. This goes substantially beyond many previous works where these pre-factors were included empirically by modifying the equation of state of the ideal electron gas [30, 35] and the Bohm potential in order to reach agreement between the QHD and the RPA results for the plasmon dispersion.

Secondly, a generalized non-local Bohm potential was derived in linear response and linked to the RPA polarization function via the second-order functional derivative of the non-interacting free energy density, Eq. (72). This has allowed us to avoid the gradient expansion entirely and, thus, constitutes a crucial step in the further improvement of QHD. In fact, this approach has allowed us subsequently to systematically include exchange-correlation contributions (terms beyond RPA) of the free energy.

Using the obtained relation, one possible non-local form of the Bohm potential was proposed in Eq. (76), making use of the ansatz Eq. (73). It is worth noting that, on the basis of Eq. (72), one may find different forms of the non-local Bohm potential by utilizing different approximations for the non-interacting free energy density functional. In the static case, as it is known from orbital-free density functional theory, there exist several different approximations, based on the relation between the second-order functional derivative of the free energy and the inverse RPA polarization func-

tion, such as a density-dependent (or independent) kernel [101], and the so-called two-point and single-point functionals [102, 103]. However, any choice of an ansatz must be checked for consistency and numerical stability [104] to avoid un-physical results.

As a third result, the exchange-correlation potential for the QHD application in linear response has been analyzed and expressed in terms of the dynamic local field correction. This has allowed us to use the result of previous studies of the dynamic local field correction in the QHD theory. In the present paper, the Bohm and exchange-correlation potentials were first considered for the case of the uniform electron gas and, after determining the potentials, for the case of a spatially varying equilibrium density. This means that, regarding an equilibrium density variation in space, the result was obtained in the adiabatic approximation. From TDDFT, it is known however, that, because of the long-ranged behavior of the exchange-correlation potential of an inhomogeneous electron system, a frequency-dependent adiabatic local density approximation does not exist [19, 23]. In other words, the exchange-correlation kernel (the second-order functional derivative of F_{xc}) is not a short-ranged function of $|\mathbf{r} - \mathbf{r}'|$. This feature is known as the ultra-non-locality problem of time-dependent DFT. However, the exchange-correlation potential in LDA can be used if the characteristic scale on which the equilibrium density distribution changes is much larger than that of the time-dependent potential [19, 105] as the exchange-correlation kernel of the homogeneous system is a short-ranged function of $|\mathbf{r} - \mathbf{r}'|$.

Information about the applicability of QHD for the description of electrons with a non-uniform equilibrium density distribution can be deduced by considering the continuity equation (67)

$$\frac{\partial n_1(\mathbf{r}, t)}{\partial t} = \nabla(n_0 \nabla w_1) = n_0 \nabla^2 w_1 \left(1 + \frac{\nabla n_0}{n_0} \frac{\nabla w_1}{\nabla^2 w_1} \right).$$

When one turns to the case of a uniform electron gas, the information about the term in brackets on the right hand

side is lost. This means that the obtained result is valid only if $\left| \frac{\nabla n_0}{n_0} \frac{\nabla w_1}{\nabla^2 w_1} \right| \ll 1$. Reformulating this condition in terms of the velocity, we obtain:

$$\left| \frac{\nabla n_0}{n_0} \right| \ll \left| \frac{\nabla \mathbf{v}}{\mathbf{v}} \right|. \quad (88)$$

The condition (88) means that the length scale of the equilibrium density variation must be much larger than the length scale of the velocity variation. Therefore, the QHD model under consideration is designated for description of quantum electrons with a weakly inhomogeneous equilibrium density distribution, but possibly, with strong correlations.

Another important point is that it is straightforward to incorporate a magnetic field into the QHD model via the minimal coupling approach, i.e. by redefining the velocity [or the scalar field w , in Eq. (8)] as $-\nabla w(\mathbf{r}, t) = \mathbf{v}(\mathbf{r}, t) \rightarrow \mathbf{v}(\mathbf{r}, t) - 1/c \mathbf{A}(\mathbf{r}, t)$, e.g. [106], where \mathbf{A} is the vector potential.

Finally, we note that the presented recipe for the consistent derivation of the quantum potential can be used for formulation of a QHD model for electrons confined in lower dimensions.

ACKNOWLEDGMENTS

We are grateful to T. Dornheim and S. Groth for helpful discussion on local field corrections. Zh.A. Moldabekov gratefully acknowledges funding from the German Academic Exchange Service (DAAD) under program number 57214224. This work has been supported by the Ministry of Education and Science of Kazakhstan under Grant No. 0263/PSF (2017).

APPENDIX A

For the partial derivative of a Hamiltonian with respect to a parameter a , the proof of the relation $\langle \frac{\partial \mathcal{H}}{\partial a} \rangle = \frac{\partial \Omega}{\partial a}$ is given in Ref. [51], where $\langle \dots \rangle$ denotes averaging over the grand canonical ensemble, and \mathcal{H} is a Hamiltonian of the system at rest and in the absence of an external field, i.e. $w = 0$ and $V_{\text{ext}} = 0$. Here we extend this relation to the case of the functional derivative $\langle \frac{\delta \mathcal{H}}{\delta n} \rangle = \frac{\delta E}{\delta n}$.

We consider the density distribution as the sum of the mean density $n_0 = \text{const}$ and the modulation $n_1(\mathbf{r})$ around n_0 , with $\int n_1(\mathbf{r}) d\mathbf{r} = 0$. The mean density n_0 is understood as the smoothed density distribution with respect to microscopic density fluctuations. The semi-

classical Hamiltonian can be expanded around n_0 as

$$\begin{aligned} \mathcal{H}[n] &= \mathcal{H}[n_0] + \int d\mathbf{r} \left. \frac{\delta \mathcal{H}[n]}{\delta n(\mathbf{r})} \right|_{n=n_0} n_1(\mathbf{r}) \\ &+ \frac{1}{2} \int \int d\mathbf{r} d\mathbf{r}' \left. \frac{\delta^2 \mathcal{H}[n]}{\delta n(\mathbf{r}, t) \delta n(\mathbf{r}') } \right|_{n=n_0} n_1(\mathbf{r}) n_1(\mathbf{r}') + \dots, \end{aligned} \quad (89)$$

from where we see that

$$\begin{aligned} \frac{\delta \mathcal{H}[n]}{\delta n(\mathbf{r})} &= \left. \frac{\delta \mathcal{H}[n]}{\delta n(\mathbf{r})} \right|_{n=n_0} \\ &+ \int d\mathbf{r}' \left. \frac{\delta^2 \mathcal{H}[n]}{\delta n(\mathbf{r}, t) \delta n(\mathbf{r}') } \right|_{n=n_0} n_1(\mathbf{r}') + \dots, \end{aligned} \quad (90)$$

where $\delta n = \delta n_1$.

Now we take into account that, for a functional of the form $F[f] = \exp \left[\int f(x) g(x) dx \right]$, the functional derivative reads

$$\frac{\delta F[f]}{\delta f} = g(x) \exp \left[\int f(x) g(x) dx \right], \quad (91)$$

and use Eqs. (89), (90), and (91) to obtain:

$$\frac{\delta}{\delta n} \left[e^{-(\mathcal{H}[n] - \mu_0 N)/T} \right] = -\frac{1}{T} \frac{\delta \mathcal{H}[n]}{\delta n} e^{-(\mathcal{H}[n] - \mu_0 N)/T}, \quad (92)$$

where T is in energy units ($k_B = 1$).

Finally, with the help of (92), we have

$$\begin{aligned} \frac{\delta E}{\delta n} &= \left\langle \frac{\delta \mathcal{H}}{\delta n} \right\rangle = e^{\Omega/T} \text{Tr} \left(e^{-(\mathcal{H}[n] - \mu_0 N)/T} \frac{\delta \mathcal{H}}{\delta n} \right) \\ &= -T e^{\Omega/T} \frac{\delta}{\delta n} \text{Tr} \left(e^{-(\mathcal{H}[n] - \mu_0 N)/T} \right) = -T e^{\Omega/T} \frac{\delta}{\delta n} e^{-\Omega/T} \\ &= -T e^{\Omega/T} \left(-\frac{1}{T} \frac{\delta \Omega}{\delta n} \right) e^{-\Omega/T} = \frac{\delta \Omega}{\delta n}. \end{aligned} \quad (93)$$

APPENDIX B

Here the convergence of the expansion (27) for the static case is discussed. This is of interest for the description of the screening of an ion by electrons as well as in the context of the construction of the non-interacting free energy density functional for orbital-free DFT applications [45].

In Fig. 4, curves of the inverse static polarization function in the RPA in units of its value at $k = 0$, $\Pi_{\text{RPA}}^{-1}(0, 0) = 2\tilde{a}_0$, are shown, for different values of the degeneracy parameter. At a fixed wavenumber, $k/2k_F > 1$, the dimensionless inverse static RPA polarization function monotonically decreases with θ , as is demonstrated in Fig. 4. In contrast, in the long wavelength limit, $k/2k_F < 1$, the dependence of $\Pi_{\text{RPA}}^{-1}(k, 0)$ on θ is non-monotonic. In this limit, with increase in the degeneracy parameter up to ~ 0.75 the value

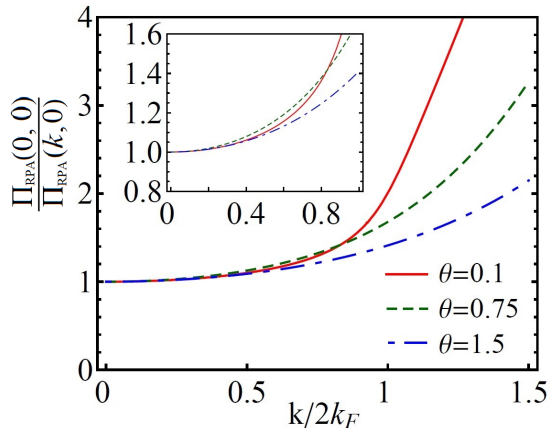


FIG. 4. The inverse value of the static polarization function in the RPA calculated in units of its value at $k = 0$, i.e., $\Pi_{\text{RPA}}^{-1}(0, 0) = 2\tilde{a}_0$ in Eq. (36), for different values of the degeneracy parameter θ .

of $\Pi_{\text{RPA}}^{-1}(k, 0)/\Pi_{\text{RPA}}^{-1}(0, 0)$ increases. In contrast, at $\theta \gtrsim$

0.75, the increase in the degeneracy parameter leads to the decrease of the dimensionless $\Pi_{\text{RPA}}^{-1}(k, 0)$.

Further, we discuss the long-wavelength limit. In Fig. 5, the convergence of the expansion, Eq. (27), for the static case, $\Pi_{\text{RPA}}^{-1}(k, 0) = 2\sum \tilde{a}_l k^l$ with the coefficients \tilde{a}_l given in Ref. [45], is demonstrated (where all odd terms are equal to zero). As is seen from Fig. (5), already the first non-zero correction, with $l = 2$, gives a good description of $\Pi_{\text{RPA}}^{-1}(k, 0)$, at $k/k_F < 1$. The agreement of the expansion with the exact curve becomes better with increase in θ . From this one can conclude that, at $\theta \sim 1$ and $k \ll 2k_F$, taking into account the first order correction, $2\tilde{a}_2 k^2$, gives already a good description of the static polarization function, at least in the case of the homogeneous electron gas. For $\theta \gtrsim 1$, the accurate interpolation of the inverse static polarization function in the RPA at $k < 2k_F$ is provided by taking into account the second non-zero correction ($l = 4$): $\Pi_{\text{RPA}}^{-1}(k, 0) = 2(\tilde{a}_0 + \tilde{a}_2 k^2 + \tilde{a}_4 k^4)$.

REFERENCES

- [1] D. Kremp, M. Schlanges, and W.D. Kraeft, Quantum Statistics of Nonideal Plasmas, (Springer 2005).
- [2] T. Sjoström, and J. Daligault, Fast and Accurate Quantum Molecular Dynamics of Dense Plasmas Across Temperature Regimes, Phys. Rev. Lett. **113**, 155006 (2014).
- [3] L. B. Fletcher *et al.*, Ultrabright X-ray laser scattering for dynamic warm dense matter physics, Nat. Phot. **9**, 274 (2015).
- [4] T. Dornheim, S. Groth, T. Sjoström, F.D. Malone, W.M.C. Foulkes, and M. Bonitz, Ab initio quantum Monte Carlo simulation of the warm dense electron gas in the thermodynamic limit, Phys. Rev. Lett. **117**, 156403 (2016).
- [5] Zh. Moldabekov, P. Ludwig, M. Bonitz, and T. Ramazanov, Ion potential in warm dense matter: Wake effects due to streaming degenerate electrons, Phys. Rev. E **91**, 023102 (2015).
- [6] Zh. Moldabekov, P. Ludwig, M. Bonitz, and T. Ramazanov, Notes on anomalous quantum wake effects, Contrib. Plasma Phys. **56**, 442 (2016).
- [7] A. I. Fernández-Domínguez, A. Wiener, F. J. García-Vidal, S. A. Maier, and J. B. Pendry, Transformation-Optics Description of Nonlocal Effects in Plasmonic Nanostructures, Phys. Rev. Lett. **108**, 106802 (2012).
- [8] A. Bennett, Influence of the electron charge distribution on surface-plasmon dispersion, Phys. Rev. B **1**, 203 (1970).
- [9] M. Marklund, G. Brodin, L. Stenflo, C.S. Liu, New quantum limits in plasmonic devices, Europhys. Lett. **84**, 17006 (2008).
- [10] C. Ciraci, and F.D. Sala, Quantum hydrodynamic theory for plasmonics: Impact of the electron density tail, Phys. Rev. B **93**, 205405 (2016).
- [11] J. J. Fortney, Characterizing the Structure of Giant Planets, Contrib. Plasma Phys. **53**, 385 (2013).
- [12] P. Haensel, A. Y. Potekhin, D. G. Yakovlev, Neutron Stars 1. Equation of State and Structure (Springer, New York 2007).
- [13] U. Zastraun *et al.*, Resolving ultrafast heating of dense cryogenic hydrogen, Phys. Rev. Lett. **112**, 105002 (2014).
- [14] O. Hurricane *et al.*, Fuel gain exceeding unity in an inertially confined fusion implosion, Nature **506**, 343 (2014).
- [15] M. E. Cuneo *et al.*, Magnetically driven implosions for inertial confinement fusion at Sandia National Laboratories, IEEE Trans. Plasma Sci. **40**, 3222 (2012).
- [16] M. R. Gomez *et al.*, Experimental demonstration of fusion-relevant conditions in magnetized liner inertial fusion, Phys. Rev. Lett. **113**, 155003 (2014).
- [17] X. Chen, *et al.*, Atomic layer lithography of wafer-scale nanogap arrays for extreme confinement of electromagnetic waves, Nature Commun. **4**, 2361 (2013).
- [18] X. Chen, C. Ciraci, D.R. Smith, and S.-H. Oh, Nanogap enhanced infrared spectroscopy with template-stripped wafer-scale arrays of buried plasmonic cavities, Nano. Lett. **15**, 107 (2015).
- [19] G.F. Giuliani and G. Vignale, Quantum Theory of the Electron Liquid (Cambridge University Press, Cambridge, 2005).
- [20] M. Bonitz, Quantum Kinetic Theory, 2nd ed. (Springer, Berlin, 2016).
- [21] P. Hohenberg, and W. Kohn, Inhomogeneous electron gas, Phys. Rev. **136**, B864 (1964).
- [22] W. Kohn and L.J. Sham, Self-Consistent Equations Including Exchange and Correlation Effects, Phys. Rev. **140**, A1133 (1965).
- [23] E. Runge and E. Gross, Density-Functional Theory for Time-Dependent Systems, Phys. Rev. Lett. **52**, 997

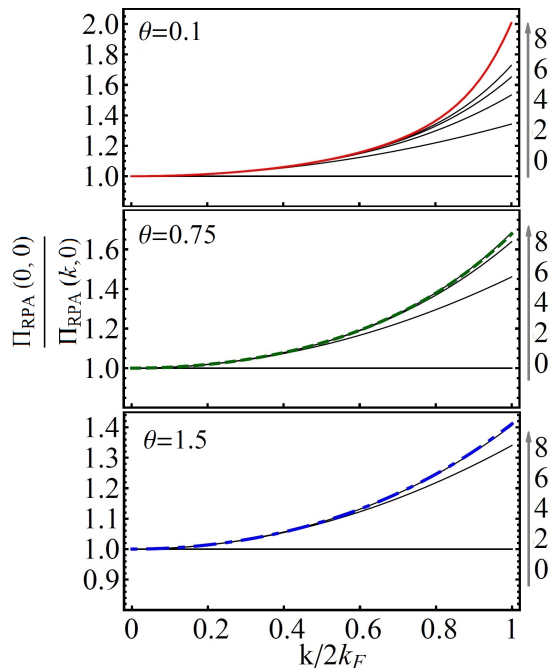


FIG. 5. Convergence of the expansion of the inverse static RPA polarization function is illustrated for the values of the degeneracy parameter 0.1, 0.75, and 1.5. Solid thin (black) curves correspond to the different maximal orders of the expansion that are included and are indicated by the numbers on the right y -axis. The explicit results for the expansion coefficients are given in Ref. [45].

- (1984).
- [24] I.V. Tokatly, Time dependent deformation functional theory, *Phys. Rev. B* **75**, 125105 (2007).
- [25] X. Gao, J. Tao, G. Vignale, I.V. Tokatly, Continuum mechanics for quantum many-body systems: Linear response regime, *Phys. Rev. B* **81**, 195106 (2010).
- [26] D. Hochstuhl, C. Hinz, and M. Bonitz, Time-dependent multiconfiguration methods for the numerical simulation of photoionization processes of many-electron atoms, *Europ. Phys. J.–Special Topics* **223**, 177-336 (2014).
- [27] M. Bonitz, Th. Bornath, D. Kremp, M. Schlanges, and W.D. Kraeft, Quantum kinetic theory for laser plasmas. Dynamical screening in strong fields, *Contrib. Plasma Phys.* **39**, 329 (1999).
- [28] K. Balzer and M. Bonitz, Nonequilibrium Green’s Functions Approach to Inhomogeneous Systems, (Springer 2013).
- [29] N. Schlünzen and M. Bonitz, *Contrib. Plasma Phys.* **56**, 5-91 (2016).
- [30] G. Manfredi, How to model quantum plasmas, *Fields Inst. Commun.* **46**, 263 (2005).
- [31] G. Manfredi, F. Haas, Self-consistent fluid model for a quantum electron gas, *Phys. Rev. B* **64**, 075316 (2001).
- [32] G. Manfredi, P.-A. Hervieux, Y. Yin, N. Crouseilles, in *Collective Electron Dynamics in Metallic and Semiconductor Nanostructures*, ed. by C. Massobrio, H. Bulou, C. Goyhenex. Atomic- Scale Modeling of Nanosystems and Nanostructured Materials, Lecture Notes in Physics, vol. 795 (Springer, Berlin, 2010).
- [33] A. Serbeto, L.F. Monteiro, K.H. Tsui, J.T. Mendonca, Quantum plasma fluid model for high-gain free-electron lasers, *Plasma Phys. Control. Fusion* **51**, 124024 (2009).
- [34] A. Kendl, P.K. Shukla, Drift wave turbulence in a dense semi-classical magnetoplasma, *Phys. Lett. A* **375**, 3138 (2011).
- [35] Wei Yan, Hydrodynamic theory for quantum plasmonics: Linear-response dynamics of the inhomogeneous electron gas, *Phys. Rev. B* **91**, 115416 (2015).
- [36] A. Jünger, *Transport Equations in Semiconductors*, (Springer, Berlin, 2009).
- [37] C.L. Gardner, The quantum hydrodynamic model for semiconductor devices, *SIAM (Soc. Ind. Appl. Math.) J. Appl. Math.* **54**, 409 (1994).
- [38] S. A. Khan, and M. Bonitz, Chapter in: Introduction to Complex Plasmas: Scientific Challenges and Technological Opportunities, M. Bonitz, K. Becker, J. Lopez, and H. Thomsen (Springer, New York, 2013), pp. 103–152
- [39] G.S. Krishnaswami, R. Nityananda, A. Sen, and A. Thyagaraja, A critique of recent semi-classical spin-half quantum plasma theories, *Contrib. Plasma. Phys.* **55**, 3 (2015).
- [40] M. Bonitz, E. Pehlke, and T. Schoof, Attractive forces between ions in quantum plasmas: Failure of linearized quantum hydrodynamics, *Phys. Rev. E* **87**, 033105 (2013).
- [41] M. Bonitz, E. Pehlke, and T. Schoof, Comment on “Discussion on novel attractive force between ions in quantum plasmas—failure of simulations based on a density functional approach”, *Phys. Scr.* **88** 057001 (2013).
- [42] N. Crouseilles, P.-A. Hervieux, G. Manfredi, Quantum hydrodynamic models for nonlinear electron dynamics in thin metal films. *Phys. Rev. B* **78**, 155412 (2008).
- [43] P. Halevi, Hydrodynamic model for the degenerate free-electron gas: Generalization to arbitrary frequencies, *Phys. Rev. B* **51**, 7497 (1995).
- [44] M. Akbari-Moghanjoughi, Hydrodynamic limit of Wigner-Poisson kinetic theory: Revisited, *Phys. Plasmas* **22**, 022103 (2015); *Erratum*, *ibid*: **22**, 039904 (2015).
- [45] Zh. Moldabekov, T. Schoof, P. Ludwig, M. Bonitz, and T. Ramazanov, Statically screened ion potential and Bohm potential in a quantum plasma, *Phys. Plasmas* **22**, 102104 (2015).
- [46] S.C. Ying, Hydrodynamic Response of Inhomogeneous Metallic system, *Il Nuovo Cimento* **23**, 270 (1974).
- [47] A. Banerjee and M.K. Harbola, Hydrodynamic approach to time-dependent density functional theory; Response properties of metal clusters, *J. Chem. Phys.* **113**, 5614 (2000).
- [48] D. Michta, F. Graziani, and M. Bonitz, Quantum Hydrodynamics for Plasmas – a Thomas-Fermi Theory Perspective, *Contrib. Plasma Phys.* **55**, 437 (2015).
- [49] D. Lurie, *Particles and Fields* (Interscience, New York, 1968).
- [50] O.A. Castro-Alvaredo, B. Doyon, and T. Yoshimura, Emergent hydrodynamics in integrable quantum systems out of equilibrium, *Phys. Rev. X* **6**, 041065 (2016).
- [51] D.N. Zubarev, Nonequilibrium Statistical Thermodynamics. (Moscow, Nauka, 1971. English translation: New York, Consultant Bureau, 1974).
- [52] J. Chihara, I. Fukumoto, M. Yamagiwa, and H. Tot-

- suji, Pressure formulae for liquid metals and plasmas based on the density-functional theory, *J. Phys.: Condens. Matter* **13**, 7183 (2001).
- [53] In Ref. [45], the notation $T[n]$ for the noninteracting free energy density functional was used instead of $F_{id}[n]$.
- [54] N. D. Mermin, Lindhard Dielectric Function in the Relaxation-Time Approximation, *Phys. Rev. B* **1**, 2362 (1970).
- [55] F. Perrot, Gradient correction to the statistical electronic free energy at nonzero temperatures: Application to equation-of-state calculations, *Phys. Rev. A* **20**, 586 (1979).
- [56] N.R. Arista and W. Brandt, Dielectric response of quantum plasmas in thermal equilibrium, *Phys. Rev. A* **29**, 1471 (1984).
- [57] A. S. Kompaneets and E. S. Pavlovskii, Self-consistent equations for atoms, *Zh. Eksp. Teor. Fiz.* **31**, 427 (1956); [*Sov. Phys.-JETP* **4**, 328 (1957)].
- [58] D. A. Kirzhnits, Quantum corrections to the Thomas-Fermi equation, *Zh. Eksp. Teor. Fiz.* **32**, 115 (1957); [*Sov. Phys.-JETP* **5**, 64 (1957)].
- [59] Y. Wang, and E.A. Carter, in *Progress in Theoretical Chemistry and Physics*, edited by S. Schwartz (Kluwer, Dordrecht, 2000), p. 117.
- [60] F. Haas and Sh. Mahmood, Linear and nonlinear ion-acoustic waves in nonrelativistic quantum plasmas with arbitrary degeneracy, *Phys. Rev. E* **92**, 053112 (2015).
- [61] W. Jones and W. H. Young, Density functional theory and the von Weizsacker method, *J. Phys. C: Solid State Phys.* **4**, 1322 (1971).
- [62] B. Eliasson and P. K. Shukla, Nonlinear quantum fluid equations for a finite temperature Fermi plasma, *Phys. Scripta* **78**, 025503 (2008).
- [63] M.L. Plumper and D.J.W. Geldart, Non-local approximation to the kinetic energy functional, *J. Phys. C: Solid State Phys.* **16**, 677 (1983).
- [64] F. Haas, G. Manfredi, M. Feix, Multistream model for quantum plasmas, *Phys. Rev. E* **62**, 2763 (2000).
- [65] J.M. Pitarke, V.M. Silkin, E.V. Chulkov, and P.M. Echenique, Theory of surface plasmons and surface-plasmon polaritons, *Rep. Prog. Phys.* **70**, 1 (2007).
- [66] C. E. Starrett, Thomas-Fermi simulations of dense plasmas without pseudopotentials, *Phys. Rev. E* **96**, 013206 (2017).
- [67] C.H. Hodges, Quantum corrections to the Thomas-Fermi approximation—the Kirzhnits method, *Can. J. Phys.* **51**, 1428 (1973).
- [68] D.R. Murphy, Sixth-order term of the gradient expansion of the kinetic energy density functional, *Phys. Rev. A* **24**, 1682 (1981).
- [69] D.J.W. Geldart and E. Sommer, Fourth-order gradient contributions in extended Thomas-Fermi theory for noninteracting fermions at finite temperature, *Phys. Rev. B* **32**, 7694 (1985).
- [70] J. Bartel, M. Brack, and D. Durand, Extended Thomas-Fermi theory at finite temperature, *Nucl. Phys. A* **445**, 263 (1985).
- [71] A. Sergeev, F.H. Alharbi, R. Jovanovic, and S. Kais, Convergent sum of gradient expansion of the kinetic-energy density functional up to the sixth order term using Padé approximant, *J. Phys: Conf. Ser.* **707**, 012011 (2016).
- [72] V.V. Karasiev, T. Sjoström, and S.B. Trickey, Generalized-gradient-approximation noninteracting free-energy functionals for orbital-free density functional calculations, *Phys. Rev. B* **86**, 115101 (2012).
- [73] T. Sjoström, and J. Daligault, Gradient correction to the exchange-correlation free energy, *Phys. Rev. B* **90**, 155109 (2014).
- [74] S. Ichimaru, Strongly coupled plasmas: high-density classical plasmas and degenerate electron liquids, *Rev. Mod. Phys.* **54**, 1017 (1982).
- [75] N.H. Kwong, and M. Bonitz, Real-time Kadanoff-Baym Approach to Nonlinear Plasma Oscillations in a Correlated Electron Gas, *Phys. Rev. Lett.* **84**, 1768 (2000).
- [76] A.A. Kugler, Theory of the local field correction in an electron gas, *J. Stat. Phys.* **12**, 35 (1975).
- [77] S. Tanaka and S. Ichimaru, Dynamic theory of correlations in strongly coupled, classical one-component plasmas: Glass transition in the generalized viscoelastic formalism, *Phys. Rev. A* **35**, 4743 (1987).
- [78] B. Dabrowski, Dynamical local-field factor in the response function of an electron gas, *Phys. Rev. B* **34**, 4989 (1986).
- [79] S. Tanaka and S. Ichimaru, Thermodynamics and correlational properties of finite-temperature electron liquids in the Singwi-Tosi-Land-Sjölander approximation, *J. Phys. Soc. Jpn.* **55**, 2278 (1986).
- [80] S. Tanaka, Improved equation of state for finite-temperature spin-polarized electron liquids on the basis of Singwi–Tosi–Land–Sjölander approximation, *Contrib. Plasma Phys.* **57**, 126 (2017).
- [81] T. Sjoström and J. Dufty, Uniform electron gas at finite temperatures, *Phys. Rev. B* **88**, 115123 (2013).
- [82] P. Vashista, and K.S. Singwi, Electron Correlations at Metallic Densities. V, *Phys. Rev. B* **6**, 875 (1972).
- [83] R.G. Dandrea, N.W. Ashcroft, and A.E. Carlsson, Electron liquid at any degeneracy, *Phys. Rev. B* **34**, 2097 (1986).
- [84] Saverio Moroni, David M. Ceperley, and Gaetano Senatore, Static Response and Local Field Factor of the Electron Gas, *Phys. Rev. Lett.* **75**, 689 (1995).
- [85] M. Corradini, R. Del Sole, G. Onida, and M. Palumbo, Analytical expressions for the local-field factor $G(q)$ and the exchange-correlation kernel $K_{xc}(r)$ of the homogeneous electron gas, *Phys. Rev. B* **57**, 14569 (1998).
- [86] S. Groth, T. Dornheim, T. Sjoström, F.D. Malone, W.M.C. Foulkes, and M. Bonitz, Ab initio Exchange-Correlation Free Energy of the Uniform Electron Gas at Warm Dense Matter Conditions, arXiv:1703.08074 *Phys. Rev. Lett.* (2017).
- [87] T. Dornheim, S. Groth, and M. Bonitz, Ab initio results for the static structure factor of the warm dense electron gas, submitted for publication to *Contrib. Plasma Phys.* (2017).
- [88] T. Dornheim, S. Groth, J. Vorberger, and M. Bonitz, Permutation Blocking Path Integral Monte Carlo approach to the Static Density Response of the Warm Dense Electron Gas, *Phys. Rev. E* **96**, 023203 (2017).
- [89] S. Groth, T. Dornheim, and M. Bonitz, Configuration Path Integral Monte Carlo approach to the Static Density Response of the Warm Dense Electron Gas, submitted for publication (2017).
- [90] Yu.V. Arkhipov, A. Askaruly, D. Ballester, A. E. Davletov, I.M. Tkachenko, and G. Zwicknagel, Dynamic properties of one-component strongly coupled plasmas: The sum-rule approach, *Phys. Rev. E* **81**, 026402 (2010).
- [91] Krishan Kumar, Vinayak Garg, and R. K. Moudgil,

- Spin-resolved correlations and ground state of a three-dimensional electron gas: Spin-polarization effects, *Phys. Rev. B* **79**, 115304 (2009).
- [92] Herwig K. Schweng and Helga M. Böhm, Finite-temperature electron correlations in the framework of a dynamic local-field correction, *Phys. Rev. B* **48**, 2037 (1993).
- [93] Priya Arora, Krishan Kumar, and R.K. Moudgil, Spin-resolved correlations in the warm-dense homogeneous electron gas, *Eur. Phys. J. B* **90**, 76 (2017).
- [94] P. Ludwig, M. Bonitz, H. Kählert, and J.W. Dufty, Dynamics of strongly correlated ions in a partially ionized quantum plasma, *J. Phys.: Conf. Series* **220**, 012003 (2010).
- [95] A. I. Fernández-Domínguez, A. Wiener, F. J. Garcá-Vidal, S. A. Maier, and J. B. Pendry, Transformation-Optics Description of Nonlocal Effects in Plasmonic Nanostructures, *Phys. Rev. Lett.* **108**, 106802 (2012).
- [96] H. Reinholz, R. Redmer, G. Röpke, and A. Wierling, Long-wavelength limit of the dynamical local-field factor and dynamical conductivity of a two-component plasma, *Phys. Rev. E* **62**, 5648 (2000).
- [97] R. Thiele, T. Bornath, C. Fortmann, A. Höll, R. Redmer, H. Reinholz, G. Röpke, and A. Wierling, S. H. Glenzer, and G. Gregori, Plasmon resonance in warm dense matter, *Phys. Rev. E* **78**, 026411 (2008).
- [98] P. Sperling, T. Liseykina, D. Bauer, and R. Redmer, Time-resolved Thomson scattering on high-intensity laser-produced hot dense helium plasmas, *New J. Phys.* **15**, 025041 (2013).
- [99] P. Neumayer *et al.*, Plasmons in Strongly Coupled Shock-Compressed Matter, *Phys. Rev. Lett.* **105**, 075003 (2010).
- [100] I. Morozov, H. Reinholz, G. Röpke, A. Wierling, and G. Zwicknagel, Molecular dynamics simulations of optical conductivity of dense plasmas, *Phys. Rev. E* **71**, 066408 (2005).
- [101] Y.A. Wang, Orbital-free kinetic-energy density functionals with a density-dependent kernel, *Phys. Rev. B* **60**, 16350 (1999).
- [102] J. Xia and E.A. Carter, Density-decomposed orbital-free density functional theory for covalently bonded molecules and materials, *Phys. Rev. B* **86**, 235109 (2012).
- [103] J. Xia and E.A. Carter, Single-point kinetic energy density functionals: A pointwise kinetic energy density analysis and numerical convergence investigation, *Phys. Rev. B* **91**, 045124 (2015).
- [104] X. Blanc, E. Cancés, Nonlinear instability of density-independent orbital-free kinetic-energy functionals, *J. Chem. Phys.* **122**, 214106 (2005).
- [105] M.K. Harbola, Differential virial theorem and quantum fluid dynamics, *Phys. Rev. A* **58**, 1779 (1998).
- [106] Adolfo Eguiluz and J. J. Quinn, Hydrodynamic model for surface plasmons in metals and degenerate semiconductors, *Phys. Rev. B* **14**, 1347 (1976).